ISBN: 978-3-95450-204-2 ISSN: 2673-5350 doi:10.18429/JACoW-IBIC2019-TUPP008

THERMAL SIMULATIONS OF OPTICAL TRANSITION RADIATION TARGETS*

J. Pforr†, M. Arnold, N. Pietralla, TU Darmstadt, Darmstadt, Germany

Abstract

The recirculating electron linac S-DALINAC provides beams with currents up to 20 µA and energies up to 130 MeV. It is planned to extend the beam diagnostics by adding multiple emittance measurement systems in order to investigate the emittance evolution along the beam line. The emittance measurement is based on the quadrupole scan technique and utilizes the existing quadrupoles and newly built optical transition radiation targets. As the targets are heated by the beam and destruction must be avoided, simulations of the thermal behaviour of the target were conducted. In particular, the dependence of the target temperature on the target design, but also variable parameters as beam spot size and current were investigated. This contribution will present these parameter studies.

NEW EMITTANCE MEASUREMENT SETUPS AT THE S-DALINAC

The S-DALINAC [1] is a thrice-recirculating electron linac. Its layout is shown in Fig. 1. In the injector, the electrons are accelerated to up to 10 MeV. Afterwards, the beam can be bent into the main accelerator, where an energy gain of 30 MeV per pass is possible. The three recirculation beam lines allow for four linac passes before the beam is extracted to the experimental hall [2].

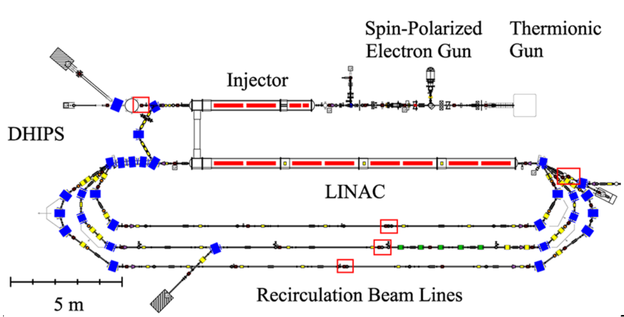

Figure 1: The layout of the S-DALINAC with three recirculation beam lines. The red boxes denote the positions of the new emittance measurement setups.

Our goal is to measure the emittance after each acceleration process. This shall allow to measure the emittance evolution along the beam line. Additionally, it would increase the reproducibility of the accelerator settings. The emittance measurement is based on a quadrupole scan [3] with optical transition radiation (OTR) targets. We installed one OTR target behind the injector, three in the recirculation beam lines and one in the extraction. Their positions are marked with red boxes in Fig. 1. For the quadrupole scan, we can use the existing quadrupoles. The targets are observed by circuit board cameras, which are installed inside lead shielding as protection from radiation damage. These cameras are used routinely for other targets as well. Alternatively, we are testing a CMOS camera (FLIR BFLY-PGE-31S4M-C) that observes the target via mirror, so that it is not in the plane of the particle accelerator and there is more lead shielding possible. This camera was mainly chosen because many parameters, e.g. exposure time and gain, can be controlled remotely.

* Work supported by DFG through GRK 2128.
† jpforr@ikp.tu-darmstadt.de

OPTICAL TRANSITION RADIATION

Transition radiation was predicted in 1947 by Ginzburg and Frank [4]. This radiation is created when a charged particle crosses the boundary between two media. The different permittivity of the media leads to a rearrangement of the electric field, and at the boundary, electromagnetic radiation is emitted. Since pioneering work was conducted in the 1970s [5], OTR is used for beam diagnostics. One advantage of OTR is that the emitted radiation is inherently proportional to the beam current, and the emission only takes place on the target surface. The emitted radiation is strongly directed, resulting in two cones of radiation in the backward halfspace, see Fig. 2. Its distribution was calculated in e.g. [6,7], but shall not be discussed here in detail. One notable aspect is the photon yield with a minimum frequency ω_{min}, that can be expressed as [8]

$$\langle N_{ph}\rangle_{\omega>\omega_{min}} \approx k\left[\left(\ln\frac{\gamma\omega_p}{\omega_{min}}-1\right)^2+\frac{\pi^2}{12}\right] \quad (1)$$

where γ is the relativistic factor, ω_p the plasma frequency and k a constant of proportionality. The plasma frequency is the oscillation frequency of electrons in the material.

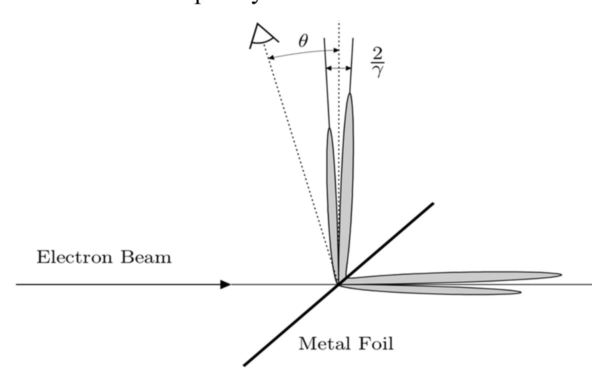

Figure 2: OTR intensity distribution for an electron beam crossing a metal foil. When the target is inclined by 45°, the radiation can be observed by a camera at 90° [9].

TARGET DESIGN

The requirements for the OTR targets include a high OTR yield, as the S-DALINAC is typically operating at

ISBN: 978-3-95450-204-2 ISSN: 2673-5350 doi:10.18429/JACoW-IBIC2019-TUPP008

beam currents of a few µA, while for the beam tuning even only 100 nA are used. In order to be sensitive enough, it is beneficial to choose a target material with

Table 1: Plasma Frequencies of Common Materials [10]

Material	Plasma Frequency [eV]
Aluminium	15
Nickel	9.45
Gold	5.8
Silver	3.735

high plasma frequency (see Eq. (1)). Table 1 shows the plasma frequencies of some materials. As aluminium has a rather high plasma frequency, we decided to use it for the OTR targets. However, due to the directed emission of OTR the target has to be mirror-like flat, as any modulation of the target surface would result in a modulation of OTR brightness. In order to achieve a sufficient flatness, we decided to use a Kapton foil, which is stretched when inserted in the target frame. This Kapton foil is coated with aluminium in order to reach a sufficient intensity. The mechanical design of the target frame results in a target foil diameter of 25 mm. The choice of the target thickness is influenced by investigations of the thermal behaviour of the target. The different thermal properties of aluminium and Kapton are summarized in Tab. 2. The higher density of aluminium results in a larger deposited power. Apart from that, aluminium conducts heat better than Kapton, but emits less energy by thermal radiation. In order to quantify the effects of target heating, conduction and emission, we simulated the thermal behaviour of the target.

Table 2: Thermal Properties of Aluminium and Kapton

	Aluminium	Kapton
Density [g/cm³]	2.7	1.4
Thermal conductivity [W/(Km)]	250	0.2
Emissivity	0.04	0.24

THERMAL SIMULATIONS

With the simulation of the target, we aimed for an estimate of the target temperature in the presence of heating by the beam, conduction and radiation. The intention of this calculation is to check the applicability of the target design and to investigate which beam parameters can be used. Kapton is expected to withstand a temperature of approx. 400 °C (670 K), so we set a limit of the target temperature at 550 K in order to have a sufficient safety margin. For the simulation, CST MPhysics Studio [11] was used. The model of our target consists of a thin foil with 25 mm diameter. This is surrounded by the target frame, which serves as a heat reservoir due to its much higher thickness. In the model, the beam is represented by a cylinder in the center of the target, where the calculated deposited beam power is uniformly distributed. The deposited power depends on the target thickness and beam current, the

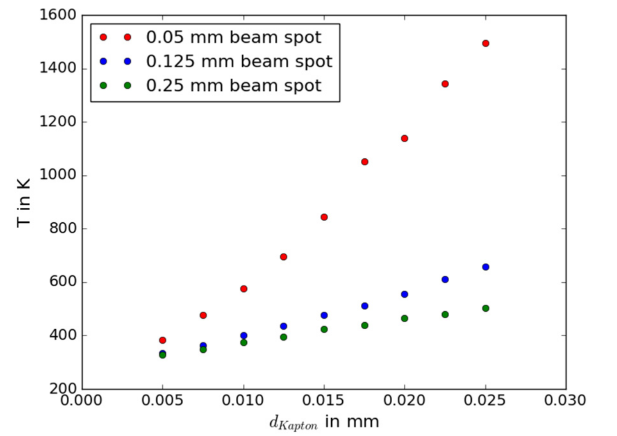

Figure 3: Maximum target temperature for a Kapton target with aluminium layer as a function of the Kapton thickness. The different colors denote different beam spot sizes, the beam current is 20 µA. Simulated with CST [11].

stopping power was estimated for typical beam energies. In order to fix the target design, we simulated the temperature distribution of the target for different target thickness and variable beam spot size. The maximum temperature as a function of the target thickness for the maximum beam current is shown in Fig. 3. From this calculation it is obvious that a thin target is thermally beneficial. We decided to use a Kapton foil thickness of 7.5 µm, as the target temperature is below 550 K even for a beam spot as small as 0.05 mm, which is a conservative estimate. With this fixed target thickness, further simulations could be conducted. A simulation of a pure Kapton target was conducted and compared to a calculation of a Kapton target with aluminium layer. The respective temperature distributions are shown in Fig. 4 and Fig. 5. In both cases, the maximum possible beam current of 20 µA and a beam spot size of 0.1 mm was used. The pure Kapton target is heated only in the beam region, but consequently the temperature rises to inacceptable high values. The simulated target temperature is far above the limit of 550 K, so destruction of the target must be expected.

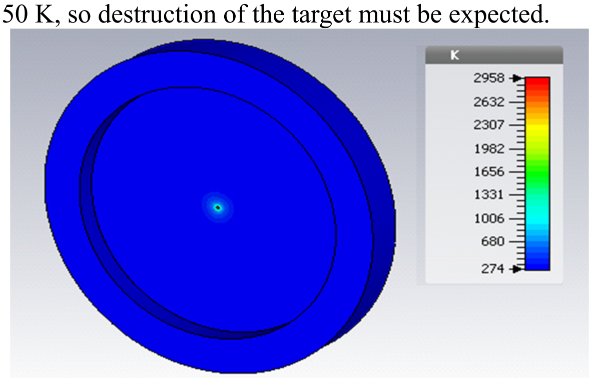

Figure 4: Temperature distribution of a Kapton target without aluminium layer for a foil diameter of 25 mm, a beam spot size of 0.1 mm and beam current of 20 µA. Simulated with CST [11].

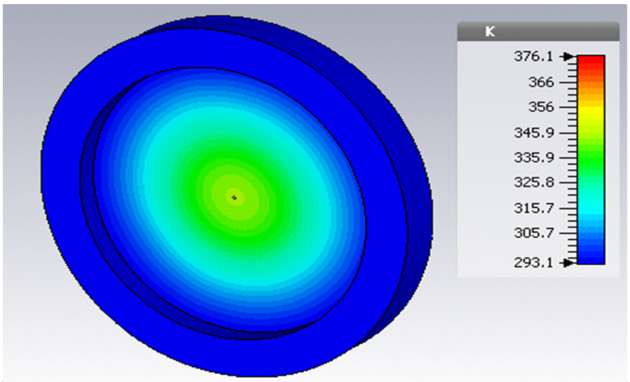

Figure 5: Temperature distribution of a Kapton target with aluminium layer for a foil diameter of 25 mm, a beam spot size of 0.1 mm and beam current of 20 µA. Simulated with CST [11].

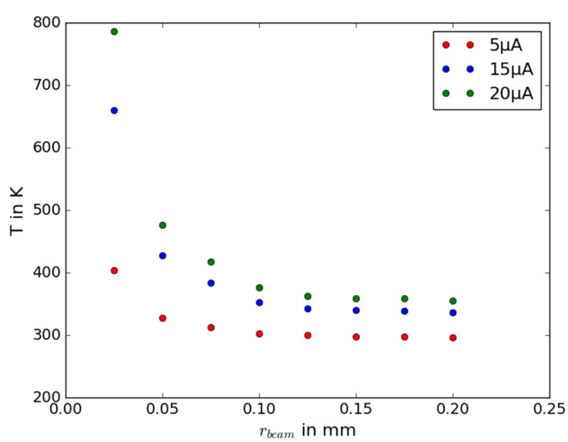

Figure 6: Maximum target temperature for a 7.5 µm thick Kapton target with aluminium layer as a function of the beam spot size. The different colors denote different beam currents. Simulated with CST [11].

An aluminium layer on the Kapton foil results in a distribution of the heat over a much larger volume. Therefore, the target is heated less, so that both Kapton and aluminium can endure the heat. So the aluminium layer is not only beneficial for the OTR yield, but improves the thermal performance significantly. However, the discussed temperatures strongly depend on the beam properties, which vary during operation. In order to quantify this dependance, the maximum target temperature was calculated for different beam spot sizes and three beam currents. The results are shown in Fig. 6. As expected, both a smaller beam spot and a higher beam current lead to a higher target temperature. The calculation shows that for the typically used beam currents of up to 5 µA even a beam spot size of 0.025 mm results in a temperature of less than 550 K. For the maximum beam current, however, such a small beam spot size would result in a destruction of the target. Therefore, measurements with OTR targets are possible at 20 µA, if one makes sure the beam spot is larger than 0.05 mm.

CONCLUSION AND OUTLOOK

For several new emittance measurement setups at the S-DALINAC, the use of OTR targets is planned. These targets consist of a 7.5 µm thick Kapton foil with additional aluminium layer. The Kapton is stretched when it is mounted in the target frame and thus provides a flat target. The aluminium increases the OTR yield and improves the thermal target behaviour. Simulations of the target temperature show that only for extreme cases of beam spot radius and beam current the target might overheat. Thus, as long as the targets are used responsibly, no damage has to be expected. Following the target design and construction, the new OTR stations have already been installed in the beam line. A previous test of this technique proved the applicability of OTR to the S-DALINAC [12]. Therefore, these stations are ready for emittance measurements in the next beamtime.

REFERENCES

[1] N. Pietralla, “The Institute of Nuclear Physics at the TU Darmstadt”, Nuclear Physics News, Vol. 28, No. 2, pp. 4-11 (2018).

[2] M. Arnold *et al.*, “Construction and Status of the Thrice Recirculating S-DALINAC”, in *Proc. 8th Int. Particle Accelerator Conf. (IPAC’18)*, Copenhagen, Denmark, May 2017, paper TUPAB030, pp. 1384-1387.

[3] H. Wiedemann, Particle Accelerator Physics, 3rd Edition, Springer, Berlin Heidelberg, 2007, doi:10.1007/978-3-319-18317-6

[4] V. L. Ginzburg and I. M. Frank, JETP 16 (1946) 15.

[5] L. Wartski, S. Roland, J. Lasalle, M. Bolore, G. Filippi, Jour. Appl. Phys. 46 (1975) 3644, doi: 10.1063/1.322092

[6] V. L. Ginzburg, V. N. Tsytovich, Several problems of the theory of transition radiation and transition scattering, Physics Reports Vol. 49, No. 1, pp. 1–89, (1979).

[7] M. L. Ter-Mikaelian, High-Energy Electromagnetic Processes in Condensed Media, Wiley-Interscience, 1972.

[8] H. Kolanoski, N. Wermes, Teilchendetektoren, Springer, 2015, doi: 10.1007/978-3-662-45350-6

[9] H. Loos, “Bestimmung der longitudinalen Struktur der Elektronenbunche im Strahl von supraleitenden Beschlleunigern”, Ph.D. thesis, Phys. Dept., TU Darmstadt, Darmstadt, Germany, 2001.

[10] D. Langley, R. A. Coutu Jr., L. A. Starman, and S. Rogers, “Optical Metamaterials for Photonics Applications”, *Proc. SPIE – The International Society of Optical Engineering*, Vol. 7468, 2009.

[11] Dassault Systemes: CST – Computer Simulation Technology AG: CST Studio Suite. Version 2016, http://www.cst.com/

[12] F. Hug, M. Arnold, T. Bahlo, J. Pforr, N. Pietralla, “Beam-based alignment of SRF cavities in an electron injector linac”, Journal of Physics: Conference Series 1067 (2018) 032021, doi: 10.1088/1742-6596/1067/3/032021